

Mississippian southern Laurentian tuffs come from a northern Gondwana arc

Hepeng Tian, Majie Fan; Victor A. Valencia; Kevin Chamberlain, Robert J. Stern, Lowell Waite

THE TUFFS

The Stanley tuffs are distributed in the Stanley Group (Fig. S1) and have been well described by Hill (1967), Niem (1977), Loomis et al. (1994), and Shaulis et al. (2012). The Beavers Bend and Hatton tuffs are in the same stratigraphic section; the lower and upper Mud Creek tuffs are in the same section; and the Chikasaw tuff is from a different section.

The Stanley tuffs have sharp lower and sharp or gradational upper contacts with shale (Niem, 1977). The lower four tuffs contain three main gradational lithologies, including a lower massive, pumiceous vitric-crystal tuff with a thin crystal-rich base, a middle bedded, pumiceous tuff, and an upper massive or bedded, fine-grained vitric tuff; the Chickasaw tuff contains only bedded vitric tuff (Niem, 1977). Phenocrysts of coarse sand-size and rip-up mud clasts up to cobble-size in the two lower units suggest these tuffs were deposited from submarine pyroclastic flows downslope from the volcano that erupted them, and the better-sorted upper unit suggests gradual setting of ashfall (Niem, 1977).

The Barnett tuff in the Permian Basin is thin, about 4-cm-thick, fine-grained, and shows sharp lower and diffusive upper contacts with shale, indicating settling of ashfall without major perturbations in the sedimentary system. The Barnett tuff was collected from a core in the center of Martin County in west Texas (Fig. S2A). The tuff resides in the lower Barnett Shale (Fig. DR 2B) based on correlation of gamma ray logs of the core and a type well (API: 42317345670000)

adjacent to the core (Mauck et al., 2018). The Barnett tuff is about 4 cm thick and is orange under ultraviolet light (Fig. S2B).

ANALYTICAL METHODS AND RESULTS

Zircon separation and morphology

Zircon grains were separated following standard procedures, including disc mill crushing, ultrasonic shaking to remove attached clays on grains, pan washing, magnetic separation and heavy liquid concentration. All the zircon grains in the tuffs were handpicked under a binocular microscope for analysis. The grains are less than 250 μm and generally euhedral and elongated (Fig. S3). Before mounting zircon grains in epoxy resin discs for geochemical analysis, over 30 grains of each sample were randomly selected and imaged using a Hitachi S3000N scanning electronic microscope (SEM) to characterize grain morphology. These grains were classified into five classes of roundness following Gärtner et al., (2013). The five classes include completely unrounded, poorly rounded, rounded, well rounded and completely rounded (Fig. S4A). Except for the upper Mud Creek tuff in the Stanley Group, more than 90% of the zircons in the other five tuffs are poorly rounded or unrounded, suggesting limited physical abrasions (Fig. S4B). The upper Mud Creek tuff has 22% of grains in the rounded and well-rounded categories.

All the zircon grains were then mounted in epoxy resin discs and polished. Representative grains were imaged using a SEM and cathodoluminescence (CL) to observe internal zoning structures and inclusions to determine spots for U-Pb age, Hf isotope analysis and rare earth element composition. Only euhedral grains were selected for analysis. Prismatic shape and internal oscillatory zoning suggest magmatic origin of grains, and small grains without oscillatory zoning likely resulted from rapid eruptive growth.

Zircon U-Pb dates and Hf isotopes by LA-ICPMS

Zircon U-Pb dates of the five Stanley tuffs and a portion of the Barnett tuff sample were measured at the Radiogenic Isotope and Geochronology Lab (RIGL) at Washington State University using an Analyte G2 193 excimer laser ablation system coupled with a Thermo-Finnigan Element 2 single-collector, inductively coupled, plasma mass spectrometer. The laser parameters were 25-35 μm in diameter spot size (depending on the size of the zircon grains), 10HZ repetition rate and $\sim 5.5 \text{ J/cm}^2$. For the U-Pb measurement, we mostly followed the method of Chang et al. (2006), except for the use of the 193nm laser system instead of the 213nm laser. A 10-second blank measurement of the He and Ar carrier gasses (Laser off) before each analysis followed by 250 scans across masses ^{202}Hg , $^{204}\text{Pb}+\text{Hg}$, ^{206}Pb , ^{207}Pb , ^{208}Pb , ^{232}Th , ^{235}U and ^{238}U during ~ 30 second laser ablation period. Analyses of zircon unknowns and quality control zircon grains were interspersed with analyses of external calibration standards, typically with 10-12 unknowns bracketed by multiple analyses of two different zircon standards (Plešovice and FC-1). The Plešovice standard (337 Ma; Sláma et al., 2008) was used to calibrate the $^{206}\text{Pb}/^{238}\text{U}$ and $^{207}\text{Pb}/^{235}\text{U}$ dates, and the FC-1 standard (1099 Ma; Paces and Miller, 1993) was used for calibration of $^{207}\text{Pb}/^{206}\text{Pb}$ dates owing to its high-count rate for ^{207}Pb (~ 2 -4 times higher than that of Plešovice). Zircon 91500 (1065 Ma; Wiedenbeck et al., 1995) and Temora2 (417 Ma; Black et al., 2004) were used as quality control standards. Data were processed offline using the Iolite software (Paton et al., 2011). Common Pb correction was performed using the ^{207}Pb method (Williams, 1998). Plots were calculated using Isoplot 4.16 (Ludwig, 2012). Zircon U-Pb data are reported in Table S1.

After the U-Pb analysis, Lu-Hf isotope compositions of selected zircon grains of the five tuffs were analyzed at the Washington State University using an Analyte G2 193nm excimer

laser ablation system coupled with a Thermo-Finnigan Neptune multi-collector mass spectrometer. Because the laser beam used for this analysis was 35-40 μm in diameter, only larger zircon grains were selected for this analysis. The laser system parameters used were laser fluence of $\sim 5.5 \text{ J/cm}^2$ and repetition rate of 10 Hz. This study used the same instrument configuration, operating parameters and data reduction methods discussed by Fisher et al. (2014), with the exception that U-Pb dates were not simultaneously determined. In this “dedicated Hf” method, the output from the ablation cell was mixed with N_2 gas and delivered directly to the Neptune MC-ICPMS. To reduce inter-laboratory bias, the Plešovice zircon standard ($^{176}\text{Hf}/^{177}\text{Hf} = 0.282482 \pm 13$, Sláma et al., 2008) was regularly analyzed between sample blocks and used to correct the measured $^{176}\text{Hf}/^{177}\text{Hf}$ of unknowns. Given the potentially large range of (Lu+Yb)/Hf in zircon samples, accurate correction for the isobaric interference of ^{176}Yb and ^{176}Lu on ^{176}Hf is imperative and should be assessed using quality control zircons interspersed with samples (Fisher et al., 2014b). Over the course of this session, five analyses of the FC-1 zircon ($^{176}\text{Hf}/^{177}\text{Hf} = 0.282184 \pm 16$, Woodhead and Hergt, 2005) yielded a $^{176}\text{Hf}/^{177}\text{Hf}$ of 0.282186 ± 44 (2SD), ten analyses of the Temora-2 zircon ($^{176}\text{Hf}/^{177}\text{Hf} = 0.282686 \pm 8$, Woodhead and Hergt, 2005) yielded a $^{176}\text{Hf}/^{177}\text{Hf}$ of 0.282694 ± 38 (2SD), and fourteen analyses of the 91500 zircons (S-MC-ICPMS $^{176}\text{Hf}/^{177}\text{Hf} = 0.282306 \pm 8$, Blichert-Toft, 2008) yielded a $^{176}\text{Hf}/^{177}\text{Hf}$ of 0.282305 ± 40 (2SD). Analyses of these quality control zircons agree well with published MC-ICPMS isotope compositions of purified Hf from these zircons, attesting to the accuracy of the interference correction methods employed.

Internal 2-sigma precision was typically $\sim 1.1 \text{ } \epsilon\text{Hf}$. Analyses with less than 25 ratios, and/or internal 2-sigma uncertainty over 2 ϵHf units were discarded and not presented here.

Present day ϵ_{Hf} values were calculated using the CHUR parameters reported by Bouvier et al. (2008). Zircon Lu-Hf data are reported in Table S2.

The U-Pb dates and Lu-Hf isotopic compositions of the remaining Barnett tuff zircons were analyzed using a laser ablation split stream (LASS) approach in which U-Pb dates and Lu-Hf isotopic compositions were determined simultaneously by coupling the single New Wave 213nm laser ablation system with the two mass spectrometers. The ablated particles were evacuated from the sample cell in a single piece of tubing, which was then split downstream into two separate paths using a “Y” connection. Each tube was attached to an individual mass spectrometer and the separated components were analyzed for different compositions concurrently. Zircon grains with fractures or small grains (less than 40 μm) were excluded from analysis. The experimental procedures follow Fisher et al. (2014). The U-Pb and Lu-Hf data of the Barnett tuff are reported in Tables S1&2.

Errors of zircon U-Pb dates and ϵ_{Hf} values are both reported as 2σ standard deviation. $^{207}\text{Pb}/^{206}\text{Pb}$ dates were interpreted for grains older than 1200 Ma and $^{206}\text{Pb}/^{238}\text{U}$ dates were interpreted for grains younger than 1200 Ma. Filters of 10% discordance and a 5% reverse discordance were applied to zircons over 500 Ma to exclude grains that may have been influenced by Pb loss or poor matrix match between samples and standards (Fig. S5). Grains less than 500 Ma were not filtered by discordance because young ICPMS dates have large $^{207}\text{Pb}/^{235}\text{U}$ uncertainty. Age plots were conducted using the Isoplot software (Ludwig, 2008) and the DZstat software (Saylor and Sundell, 2016).

Zircon U-Pb date of the Barnett tuff by CA-ID-TIMS

After the U-Pb and Lu-Hf analyses, seven zircons in the youngest group of the Barnett tuff were analyzed by chemical abrasion, isotope dilution, thermal ionization mass spectrometry (CA-ID-TIMS) at the University of Wyoming. These grains were plucked from the epoxy mount after LA-ICP analysis and selected to test whether the range of dates from LA-ICP was robust or was an artifact of Pb loss and matrix mismatch. Zircon dissolution and chemistry were adapted from methods developed by Parrish et al. (1987) and Mattinson (2005). Zircon grains were chemically abraded by annealing them for 50 hours at 850°C and partially dissolving them in HF and HNO₃ acids for 12 hours at 180°C. Single zircon grains were then spiked with a mixed ²⁰⁵Pb/²³³U/²³⁵U tracer (ET535), dissolved in HF and HNO₃ at 235 °C for 30 hours, and converted to chlorides at 180 °C for 16 hours. Dissolved zircon samples were loaded onto single rhenium filaments with silica gel and H₃PO₄ without any further chemical processing. Isotopic compositions were measured on a Micromass Sector 54 mass spectrometer in single-collector, peak-switching mode using the Daly-photomultiplier collector for all isotopes. Mass discrimination of 0.25 ± 0.10 %/amu for Pb was determined by replicate analyses of NIST SRM 981. UO₂ fractionation was determined internally and corrected for oxide interference. Pb blank averaged <1 pg for zircons. Isotopic composition of the Pb blank was measured as 18.572 ± 0.39 , 15.731 ± 0.43 , and 38.380 ± 0.97 for ²⁰⁶Pb/²⁰⁴Pb, ²⁰⁷Pb/²⁰⁴Pb and ²⁰⁸Pb/²⁰⁴Pb, respectively. U blanks were consistently less than 0.01 pg. Concordia coordinates, intercepts, and uncertainties were calculated using PBMacDAT and ISOPLOT programs (based on Ludwig 1988, 1991); initial Pb isotopic compositions were estimated from the Stacey and Kramers (1975) model. ²⁰⁶Pb/²³⁸U and ²⁰⁷Pb/²⁰⁶Pb ratios and dates were corrected for Th-disequilibrium after Schärer (1984) assuming a magma Th/U of 2.2. The decay constants used by PBMacDAT and ISOPLOT are those recommended by the I.U.G.S. Subcommittee on Geochronology (Steiger and Jäger, 1977),

including $0.155125 \times 10^{-9}/\text{yr}$ for ^{238}U , $0.98485 \times 10^{-9}/\text{yr}$ for ^{235}U and 137.88 for present-day $^{238}\text{U}/^{235}\text{U}$ ratio. Precision of the weighted mean $^{206}\text{Pb}/^{238}\text{U}$ date is reported in the $\pm X/Y/Z$ format of Schoene et al., (2006), with X as the analytical uncertainty (95% confidence), Y includes tracer calibration uncertainties for comparisons to other U-Pb dates, and Z includes U decay uncertainties for comparison to dates from other systems as long as the uncertainties of those dates have been fully propagated. Zircon U-Pb data of the CA-ID-TIMS analyses are reported in Table S3.

Youngest mode weighted mean date

Many detrital zircon studies have been conducted to evaluate methods of the maximum depositional ages using LA-ICPMS dates (e.g., Spencer et al., 2016; Coutts et al., 2019; Herriot et al., 2019). We modified the youngest statistical population (YSP) approach from Coutts et al. (2019) which selects the negative tail of the youngest population of LA-ICPMS dates (≥ 2) and calculates the weighted mean of their dates with a mean square weighted deviation (MSWD) near 1. A recent study of Jurassic volcanoclastic strata in Alaska shows that the YSP approach yields the best coincidence with CA-ID-TIMS dates (Herriot et al., 2019). Because our samples are volcanic tuffs, the youngest dominant population, which is the YSP, should be from a single eruptive event. We calculate the age of each tuff using the mode of YSP in the kernel density estimation (KDE) plot (Fig. 2A). The age was calculated as the weighted mean of more than three grains overlapping at 2σ and has a mean square weighted deviation (MSWD) near 1. This method excludes ICPMS dates at both tails of the distribution that do not overlap at 2σ with the mode. These scattered dates typically reflect Pb loss, matrix effect-related bias, and inheritance of grains from the magma source (e.g., Schaltegger et al., 2015).

Our youngest mode weighted mean date of the Barnett tuff matches the CA-ID-TIMS date well, indicating that this approach yields accurate tuff ages. Our youngest mode dates of the Beavers Bend, Lower Mud Creek, and Chickasaw tuffs are consistent with the results from Shaulis et al., (2012) using the same statistical approach, but produced higher precision (Table DR5). Our method dates the Hatton tuff to 317.4 ± 0.5 Ma ($n = 48$), which is younger than the date (324.8 ± 2.5 Ma; $n = 9$) reported in Shaulis et al. (2012). The Hatton tuff date is also younger than the lower Mud Creek and Chickasaw tuff dates. These differences suggest either that the earlier stratigraphy is incorrect and the Hatton tuff is the youngest Stanley tuff, or that there are minor unresolved age biases in some of these data sets.

Dates older than 350 Ma

In all tuffs, grains older than 350 Ma are mostly clustered at 350-500 Ma, 500-850 Ma, 900-1300 Ma, and 1300-1600 Ma (Fig. S6). The zircon ICPMS dates of the upper Mud Creek tuff cluster at <330 Ma (4%), 350-500 Ma (49%), 500-850 Ma (7%), 900-1300 Ma (27%) and 1300-1600 Ma (13%). The composite U-Pb data of the other four Stanley tuffs are mostly <350 Ma (91%) with a few grains in the other clusters, including 350-500 Ma (3%), 500-850 Ma (2%), and 900-1300 Ma (4%). The Barnett tuff also has abundant grains <350 Ma (68%), with other grains in the clusters of 350-500 Ma (6%), 500-850 Ma (6%), 900-1300 Ma (15%) and 1300-1600 Ma (2%).

Zircon Rare Earth Element Analyses

Zircons large enough to accommodate another laser ablation spot were selected for rare earth element analysis at the Washington State University using the same LA-ICP-MS instrument used for Lu-Hf isotope analysis. New laser spots were placed within the same zone

for U-Pb and Lu-Hf isotope analyses. Each analysis consists of two cleaning pulses, followed by 10 seconds of washout, 18 seconds of gas blank, and 40 seconds ablation time followed by 15 seconds of waiting time before moving the stage. Three standards, including NIST610 and NIST612 (both are synthetic glass standards) and zircon reference 91500, were dispersed every 15 analyses. Correction and data reduction were carried out using the Iolite Software (Woodhead et al, 2007). The trace element analytical data are summarized in Figure S7 and reported in Table S4.

DISCUSSION OF OLD GRAINS

The upper Mud Creek tuff has 22% of grains in the rounded and well-rounded categories (Fig. DR4), suggesting physical abrasion through sediment transport. The sample has only three grains < 330 Ma suggesting that the tuff contains detrital grains in the depositional system and possibly inherited grains from the magma source. About 50% of the grains are in the 350-500 Ma group, which is significantly more than those in sandstone of the Stanley Group (Fig, DR6; Prine, 2020). Grains of these ages are both abundant in upper Paleozoic in the Appalachian foreland on Laurentia, representing the Acadia and Taconic orogenies (e.g., Thomas et al., 2017), and in Mexico that was on Gondwana during the late Paleozoic, such as the Mississippian Lower Santa Rosa Formation in southeastern Mexico (Weber et al., 2009) and magmatism of 410-370 Ma in the Acatlan Complex, southern Mexico (Yañez et al., 1991). Although Paleozoic grains have been suggested to be transported from the Appalachians into the Arkoma shelf by a large transcontinental river (e.g., Wang and Bidgoli, 2019), the age distribution of the upper Mud Creek tuff is very different from that of the Stanley sandstone that is representative to the zircon age signature of the deep-water depositional environment in Laurentia margin. Therefore, Paleozoic grains in the upper Mud Creek tuff were most likely recycled from the approaching

peri-Gondwana terranes and/or inherited from the inferred Gondwana arc. The other four Stanley tuffs, including the Beavers Bend, Hatton, lower Mud Creek and Chickasaw tuffs, have only <10% grains older than 350 Ma that are detrital and/or inherited.

Both the Barnett and four Stanley tuffs have old grains clustered at 350-500 Ma, 500-850 Ma, and 900-1300 Ma. The 900-1300 Ma zircons were ultimately from the Grenville basement that was distributed in the Appalachians and western Texas on Laurentia, and in Peri-Gondwana terranes (e.g., Lopez et al., 2001; Thomas et al., 2017). The 500-850 Ma zircons are characteristic of Peri-Gondwana or Gondwana source as these grains were ultimately from the Pan-African and Brasiliano orogeny on Gondwana (e.g., Weber et al., 2009). Given that Laurentia-Gondwana collision had not extended to Texas during the Mississippian, the presence of 500-850 Ma age group in these tuffs suggests that some, if not all, of the old grains in the tuffs were most likely inherited from the inferred Gondwana arc.

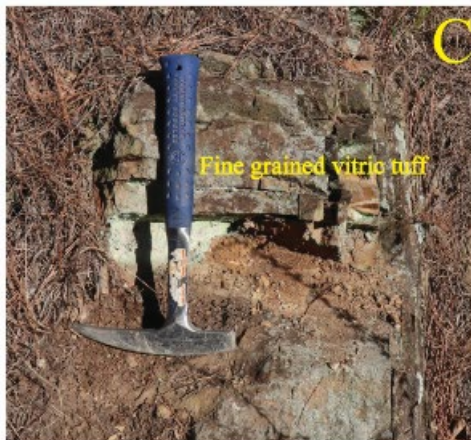
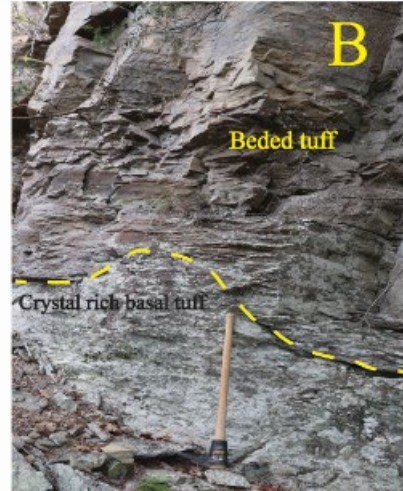
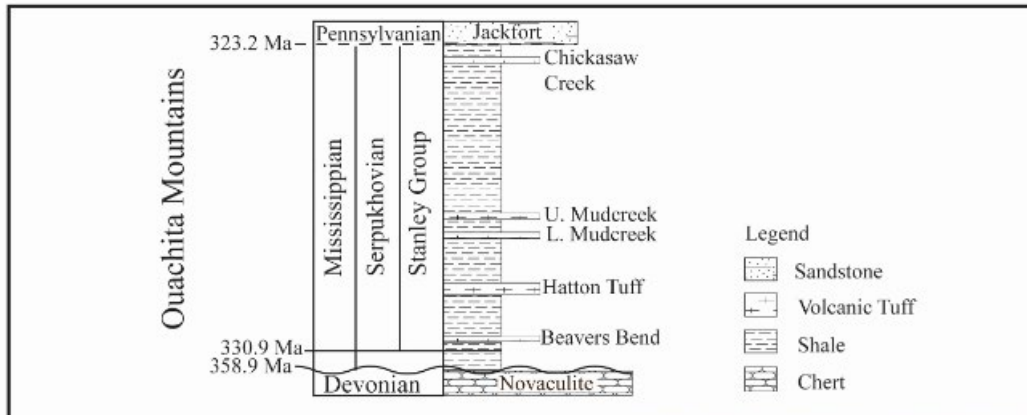


Figure S1. Stratigraphic column of the Stanley Group in the Ouachita Mountains showing the stratigraphic levels of the five studied tuffs (modified after Shaulis et al., 2012) and field photos of the tuffs. A). The Beavers Bend tuff (34.135064, -94.676459); B). The Hatton tuff

(34.135056, -94.676472); C). The lower Mud Creek tuff (34.313572, -94.820431); and D). The Chickasaw Creek tuff (34.73169, -93.35568). Note that the upper Mud Creek tuff was collected at the same location as the lower Mud Creek tuff.

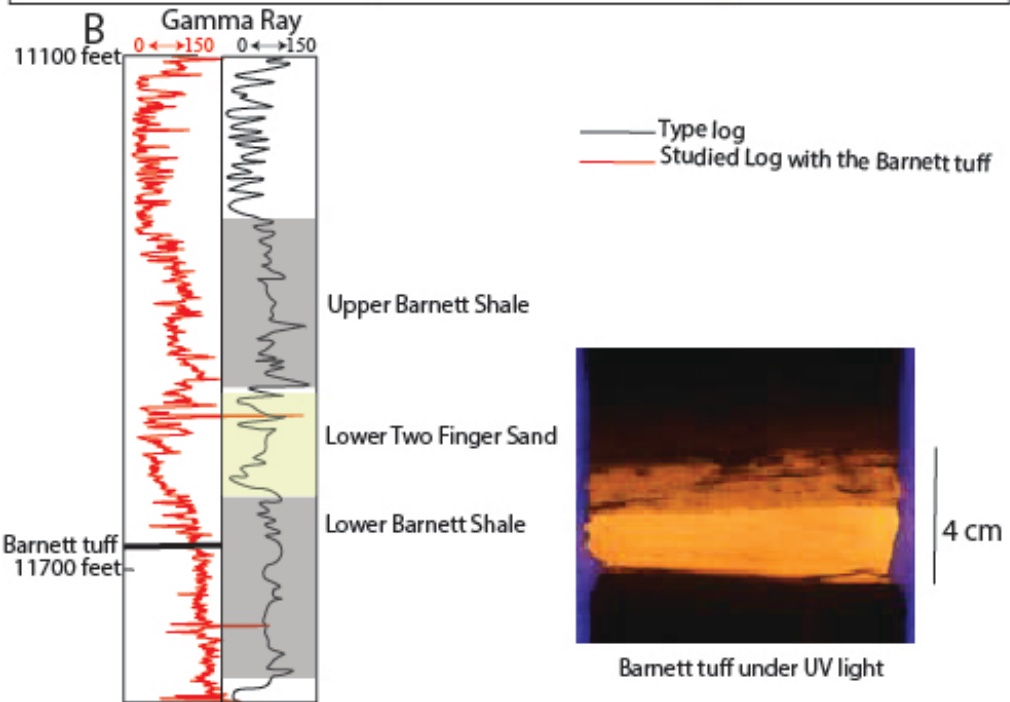
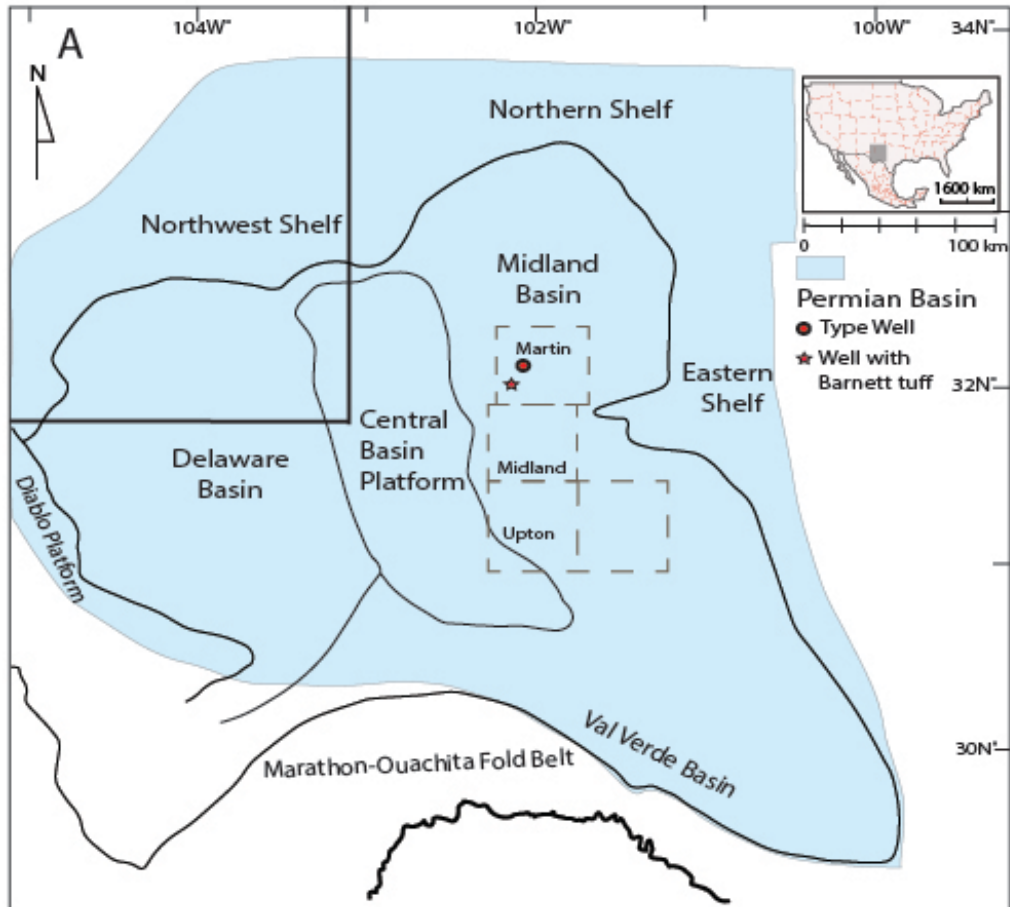


Figure S2. A) Locations of the Midland Basin in west Texas and our studied core and the type log in Martin County. B) Gamma ray log correlation of our studied core containing the Barnett tuff and the type log in Mauck et al. (2018). Note that the sharp lower boundary and diffusive upper boundary of the Barnett tuff in our studied core. The tuff is not recognized in the type log.

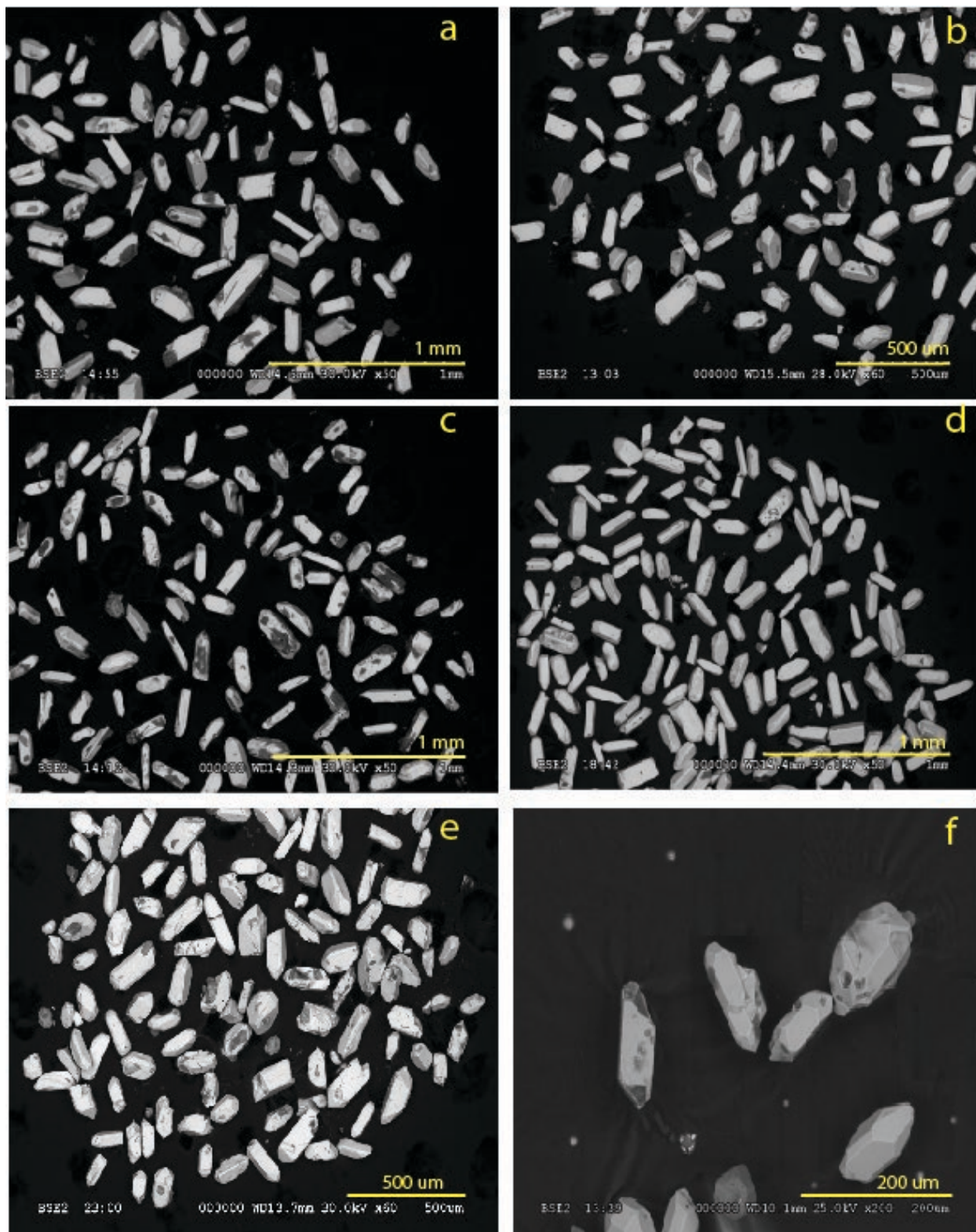


Figure S3. Scanning Electron Microscope images of the zircons from the Stanley tuffs and the Barnett tuff. A. Beavers Bend tuff; B) Hatton tuff, C) Lower Mud Creek tuff; D) Upper Mud Creek tuff; E) Chickasaw Creek tuff; and F) Barnett tuff.

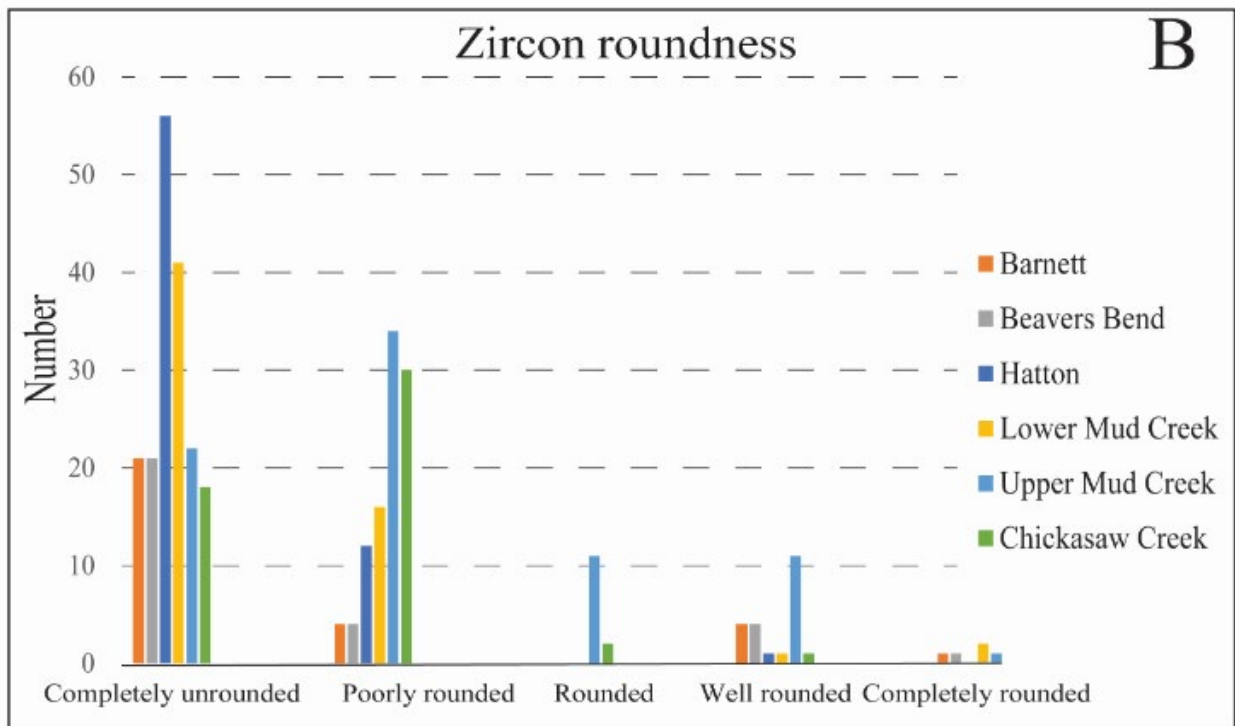
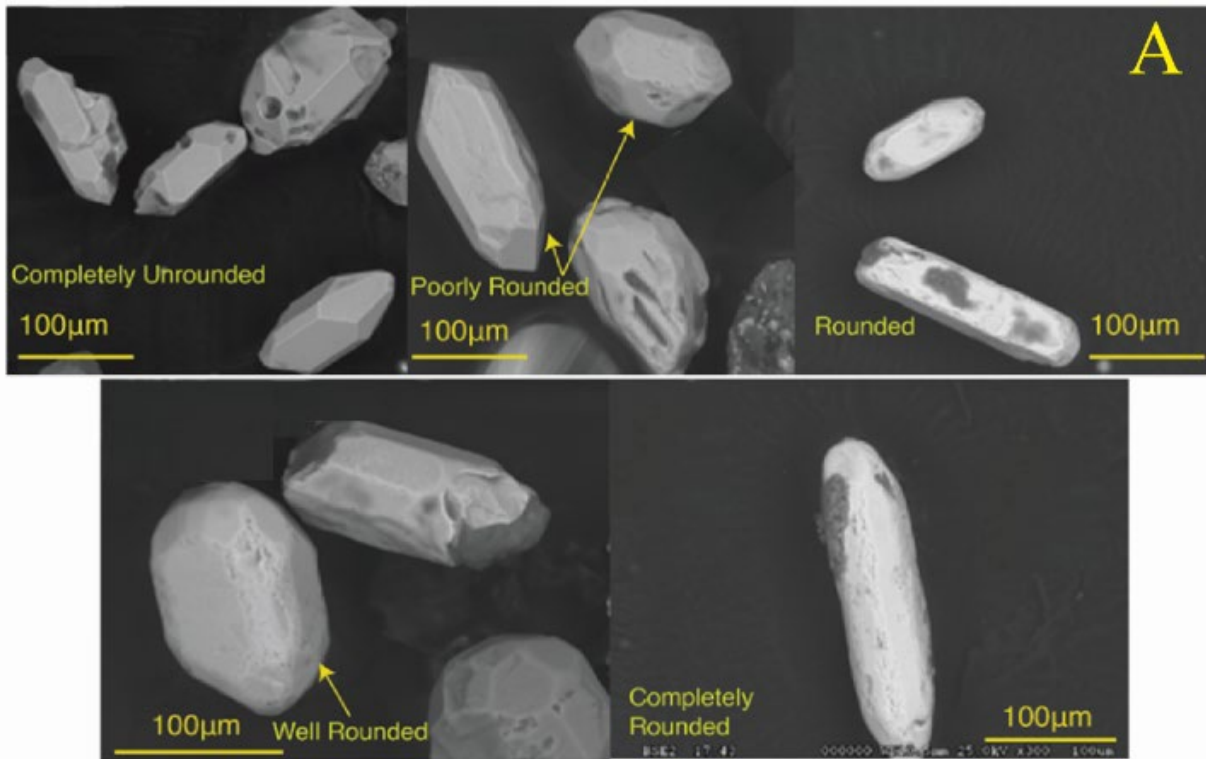


Figure S4. A) Pictures of representative grains for five roundness categories. B) Plot shows roundness data for zircons from all the tuffs. Note that zircons that are rounded, well rounded and completely rounded were filtered out for dating.

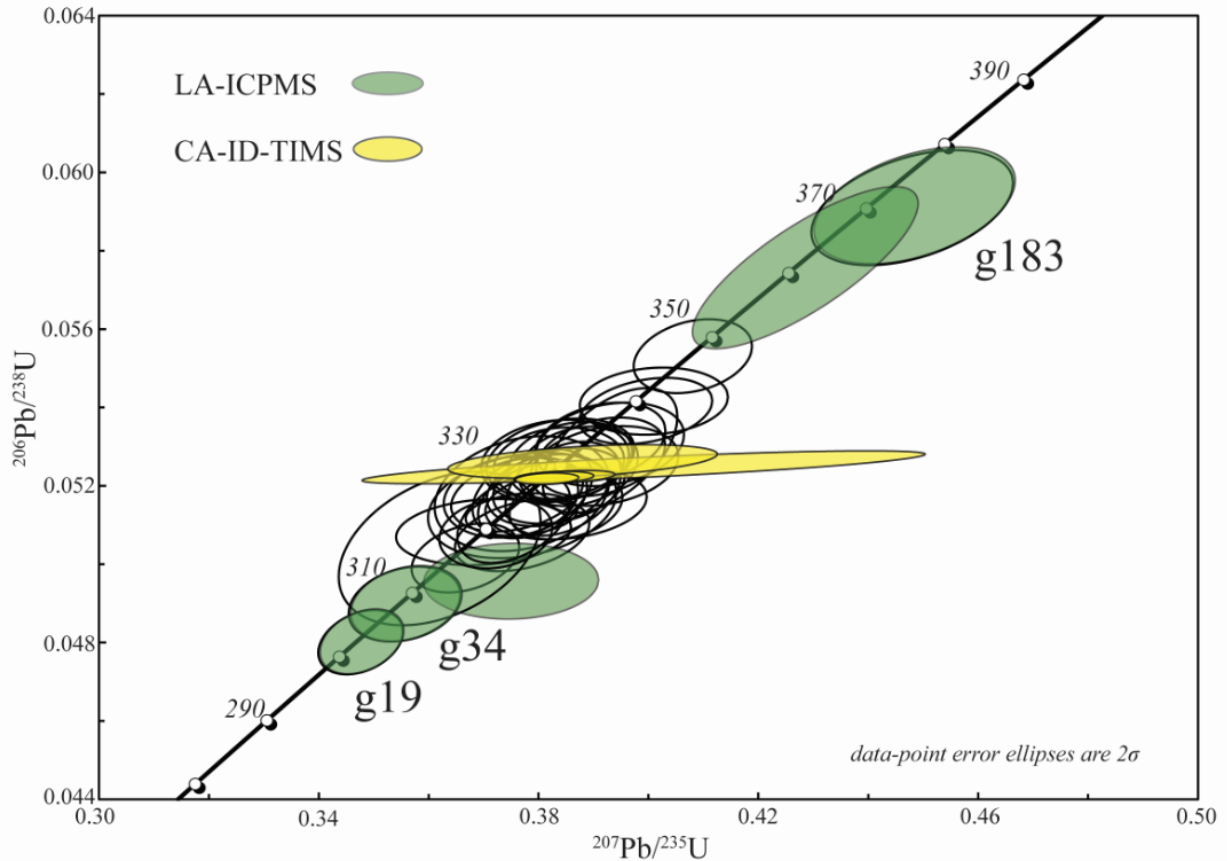


Figure S5. Concordia plot for LA-ICPMS dates vs. CA-ID-TIMS dates for the Barnett tuff. Grains that produced the green-filled ellipses were plucked from the ICP mount and analyzed by CA-ID-TIMS (yellow ellipses), thereby directly comparing the two dating methods. The observation that all the CA-ID-TIMS dates form a single tight cluster strengthens our confidence that the ages of the zircons are ca. 328 Ma and that the variation within the LA-ICPMS dates is due to either Pb loss (g19, g34, and all others that are younger than the TIMS dates) or matrix mismatch, which can produce dates that are anomalously old (e.g., Schaltegger et al., 2015; g183 and the others that are older than the TIMS dates). The YSP of the LA-ICPMS date is 327 Ma despite the large overall variation. The agreement between YSP from the LA-ICPMS date and the CA-ID-TIMS date in this sample adds to evidence from other direct comparative studies of the two methods (e.g., Herriott et al., 2019; Coutts et al., 2019) and supports interpreting the YSPs as the best estimates for MDAs from LA-ICPMS data.

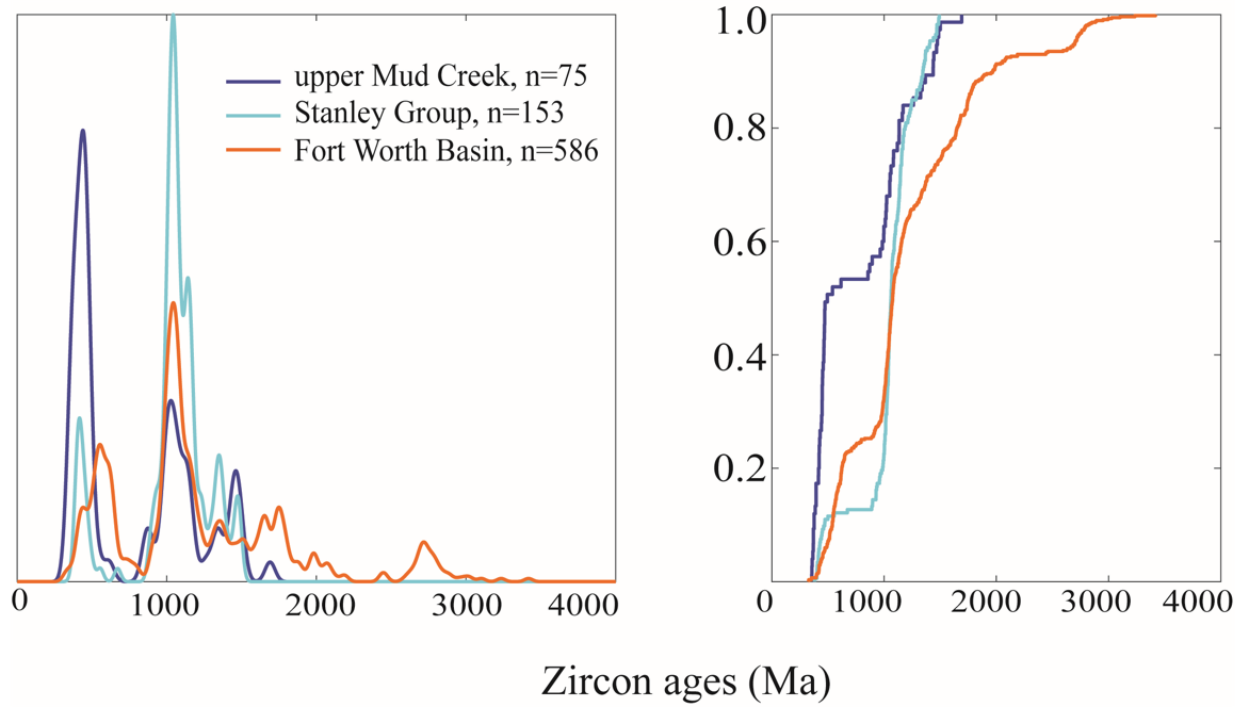


Figure S6. Zircon age KDE plots and cumulative distribution function plots for the upper Mud Creek tuff, Late Mississippian sandstone in the Stanley Group (Prine, 2020) and Middle Pennsylvanian sandstone in the Fort Worth Basin in northern Texas (Alsalem et al., 2018).

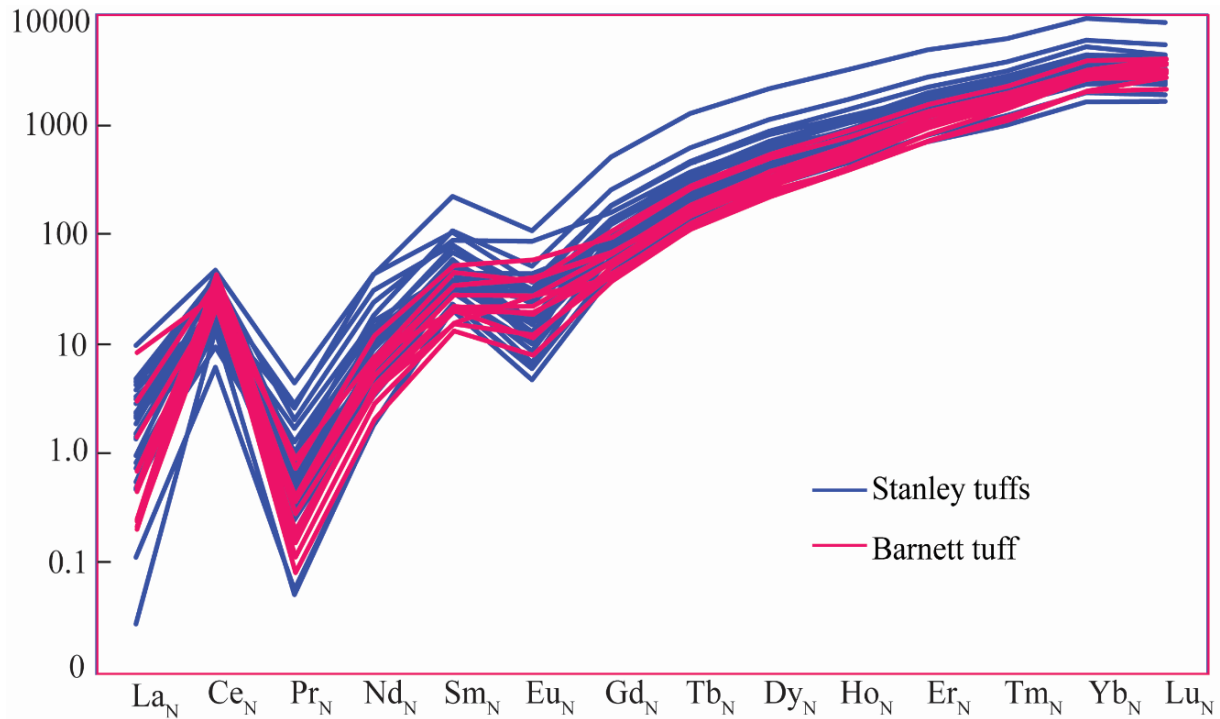


Figure S7. Zircon REE patterns normalized to Chondrite after McDonough and Sun (1995).

Table S5. Zircon U-Pb ages derived from LA-ICPMS dates of the Stanley and Barnett tuffs

Tuff		N analyzed	Date (Ma)	$\pm 2\sigma$	n	MSWD	PoF
Chickasaw Creek	this study	81	320.4	0.8	30	0.8	0.8
	Shaulis et al. (2012)	77	320.1	1.7	18	1.1	0.4
Upper Mud Creek	this study	78	N/A				
	Shaulis et al. (2012)	94	322.7	2.3	13	1	0.5
Lower Mud Creek	this study	115	320.7	0.6	50	1	0.4
	Shaulis et al. (2012)	70	322.3	1.7	22	0.6	0.9
Hatton	this study	103	317.4	0.5	48	1	0.5
	Shaulis et al. (2012)	88	324.8	2.5	9	1	0.4
Beaver Bend	this study	112	327.1	0.7	34	1	0.5
	Shaulis et al. (2012)	84	327.3	2.3	15	1	0.5
Barnett Tuff	this study	252	326.7	0.6	52	0.9	0.7
	CA-ID-TIMS	7	327.8	0.8	5	1.2	0.1

The upper Mud Creek tuff only yields 3 zircon dates within 350 Ma, not enough for calculating the weighted mean age.

References

- Alsalem, O.B., Fan, M., Zamora, J., Xie, X. and Griffin, W.R., 2018, Paleozoic sediment dispersal before and during the collision between Laurentia and Gondwana in the Fort Worth Basin, USA: *Geosphere*, v. 14, p. 325–342.
- Black, L.P., Kamo, S.L., Allen, C.M., Davis, D.W., Aleinikoff, J.N., Valley, J.W., Mundil, R., Campbell, I.H., Korsch, R.J., Williams, I.S., and Foudoulis, C., 2004, Improved Pb-206/U-218 microprobe geochronology by the monitoring of a trace-element-related matrix effect; SHRIMP, ID-TIMS, ELA-ICP-MS and oxygen isotope documentation for a series of zircon standards: *Chemical Geology*, v. 205, p. 115-140.
- Blichert-Toft, J., 2008, The Hf isotopic composition of zircon reference material 91500: *Chemical Geology*, v. 253, p. 252-257.
- Bouvier, A., Vervoort, J.D., Patchett, P.J., 2007, The Lu-Hf and Sm-Nd isotopic composition of CHUR: constraints from unequilibrated chondrites and implications for the bulk composition of terrestrial planets: *Earth and Planetary Science Letters*, v 219, p. 311.
- Chang, Z., Vervoort, J.D., McClelland, W.C., and Knaack, C., 2006, U-Pb dating of zircon by LA-ICP-MS: *Geochemistry, Geophysics, Geosystems*, v.7, p.1-14, doi: 10.1029/2005GC001100.
- Coutts, D.S., Matthews, W.A., and Hubbard, S.M., 2019, Assessment of widely used methods to derive depositional ages from detrital zircon populations: *Geosci-ence Frontiers*, v.10, no. 4, p.1421–1435, <https://doi.org/10.1016/j.gsf.2018.11.002>.
- Fisher, C.M., Hanchar, J.M., Samson, S.D., Dhuime, B., Blichert-Toft, J., Vervoort, J.D., and Lam, R., 2011, Synthetic zircon doped with hafnium and rare earth elements _ A reference material for in situ hafnium isotope analysis _ Elsevier Enhanced Reader.pdf: *chemica*, v. 286, p.32–47.
- Fisher, C.M., Vervoort, J.D., and Dufrane, S.A., 2014, Accurate Hf isotope determinations of complex

zircon using the “laser ablation split stream” method: *Geochemistry, Geophysics, Geosystems*, v. 15, p.121–139, doi: 10.1002/2013GC004962.

Herriott, T. M., Crowley, J. L., Schmitz, M. D., Wartes, M. A., & Gillis, R. J. (2019). Exploring the law of detrital zircon: LA-ICP-MS and CA-TIMS geochronology of Jurassic forearc strata, Cook Inlet, Alaska, USA: *Geology*, v. 47, p.1044–1048, <https://doi.org/10.1130/G46312.1>

Hill, J.G., 1967, Sandstone petrology and stratigraphy of the Stanley Group (Mississippian), southern Ouachita Mountains, Oklahoma [PhD thesis]: Madison, University of Wisconsin, 106 p.

Loomis, J., Weaver, B., and Blatt, H., 1994, Geochemistry of Mississippian tuffs from the Ouachita Mountains, and implications for the tectonics of the Ouachita Orogen, Oklahoma and Arkansas: *Geological Society of America Bulletin*, v. 106, p. 1158–1171, doi: 10.1130/0016-7606(1994)106<1158:GOMTFT>2.3.CO;2.

Lopez, R., Cameron, K.L., Jones, N.W., 2001, Evidence for Paleoproterozoic, Grenvillian, and Pan-African age Gondwanan crust beneath northeastern Mexico, *Precambrian Research*, v. 107, p.195-214, [https://doi.org/10.1016/S0301-9268\(00\)00140-6](https://doi.org/10.1016/S0301-9268(00)00140-6).

Ludwig, K.R., 2008, User’s Manual for Isoplot 3.70: Berkeley Geochronology Center Special Publication, p.76.

Ludwig, K.R., 1988, PBDAT for MS-DOS, a computer program for IBM-PC compatibles for processing raw Pb-U-Th isotope data, version 1.24: U.S. Geological Survey, Open-File Report 88-542, 32 pp.

Ludwig, K.R., 1991, ISOPLOT for MS-DOS, a plotting and regression program for radiogenic-isotope data, for IBM-PC compatible computers, version 2.75: U.S. Geological Survey, Open-File Report 91-445, 45 pp.

Mauck, J.V., Loucks, R.G., Entzminger, D.J., 2018, Stratigraphic Architecture, Depositional Systems,

and Lithofacies of the Mississippian Upper Barnett Two Finger Sand Interval, Midland, Basin, Texas: Gulf Coast Association of Geological Societies. v.7, p.21-45, doi: 10.26153/tsw/9455.

McDonough, William & Sun, S.S.. 1995, The composition of the Earth: *Chemical Geology*, v.67, p.1050-1056.

Mattinson, J.M, 2005, Zircon U-Pb chemical abrasion (“CA-TIMS”) method: combined annealing and multi-step partial dissolution analysis for improved precision and accuracy of zircon ages: *Chemical Geology*, v.220, p.47-66.

Niem, A.R., 1977, Mississippian pyroclastic flow and ash-fall deposits in the deep-marine Ouachita flysch basin, Oklahoma and Arkansas: *Geological Society of America Bulletin*, v.88, p.49–61.

Paces, J.B., and Miller Jr, J.D., 1993, Precise U-Pb ages of Duluth Complex and related mafic intrusions, northeastern Minnesota: Geochronological insights to physical, petrogenetic, paleomagnetic, and tectonomagmatic processes associated with the 1.1 Ga Midcontinent Rift System: *Journal of Geophysical Research*, v. 98, p. 13997-14013.

Paton, C., Hellstrom, J., Paul, B., Woodhead, J. and Hergt, J., 2011. Iolite: Freeware for the visualisation and processing of mass spectrometric data: *Journal of Analytical Atomic Spectrometry*, v.26, p. 2508-2518.

Parrish, R.R., Roddick, J.C., Loveridge, W.D., and Sullivan, R.D., 1987, Uranium-lead analytical techniques at the geochronology laboratory, Geological Survey of Canada, in *Radiogenic age and isotopic studies, Report 1: Geological Survey of Canada Paper 87-2*, p.3–7.

Prines, S.T., 2020, U-Pb Detrital Zircons of the Syn-orogenic Carboniferous Deep-water Clastic Deposits in the Ouachita Mountains, Arkansas, United States [M.S. Thesis]: Texas Christian University, 80 p.

Saylor, J.E. and Sundell, K.E., 2016, Quantifying comparison of large detrital geochronology data sets:

Geosphere, v.12, p.203-220.

Schaltegger, U., Schmitt, A.K., Sciences, S., Angeles, L., Survey, B.G., and Schaltegger, U., 2015, U-Th-Pb zircon geochronology by ID-TIMS, SIMS, and laser ablation ICP-MS: recipes, interpretations, and opportunities: *Chemical Geology*, v. 402, p. 89–110, doi: <https://doi.org/10.1016/j.chemgeo.2015.02.028>.

Schoene, B., Crowley, J.L., Condon, D.J., Schmitz, M.D. and Bowring, S.A., 2006. Reassessing the uranium decay constants for geochronology using ID-TIMS U–Pb data: *Geochimica et Cosmochimica Acta*, 70(2), pp.426-445.

Sláma, J., Košler, J., Condon, D.J., Crowley, J.L., Gerdes, A., Hanchar, J.M., Horstwood, M.S.A., Morris, G.A., Nasdala, L., Norberg, N., Schaltegger, U., Schoene, B., Tubrett, M.N., and Whitehouse, M.J., 2008, Plešovice zircon — A new natural reference material for U–Pb and Hf isotopic microanalysis: *Chemical Geology* v. 249, p. 1-35.

Stacey, J.S. and Kramers, J.D., 1975, Approximation of terrestrial lead isotope evolution by a two-stage model: *Earth and Planetary Science Letters*, v. 26, p.207–221.

Steiger, R.H. and Jäger, E., 1977, Subcommittee on geochronology: convention on the use of decay constants in geo- and cosmochronology: *Earth and Planetary Science Letters*, v. 36, p.359-362.

Thomas, W.A., Gehrels, G.E., Greb, S.F., Nadon, G.C., Satkoski, A.M., and Romero, M.C., 2017, Detrital zircons and sediment dispersal in the Appalachian foreland: *Geosphere*, v. 13, no. 6, p. 2206–2230, doi:10.1130/GES01525.1.

Wang, W., and Bidgoli, T., 2019, Detrital Zircon Geochronologic Constraints on Patterns and Drivers of Continental-Scale Sediment Dispersal in the Late Mississippian: *Geochemistry, Geophysics, Geosystems*. v.20, p. 5522-5543, 10.1029/2019GC008469.

Weber, B., Valencia, V.A., Schaaf, P., and Ortega-Gutiérrez, F., 2009, Detrital zircon ages from the Lower Santa Rosa Formation, Chiapas: Implications on regional Paleozoic stratigraphy:

Revista Mexicana de Ciencias Geológicas, v. 26, no. 1, p. 260–276.

Wiedenbeck, M., Allé, P., Corfu, F., Griffin, W.L., Meier, M., Oberli, F., Von Quadt, A., Roddick, J.C., and Spiegel, W., 1995, Three natural zircon standards for U-Th-Pb, Lu-Hf, trace element and REE analyses: *Geostandards Newsletters*, v. 19, p. 1-23.

Williams, I.S., 1998, U-Th-Pb geochronology by ion microprobe: M.A. McKibben, W.C. Shanks III, W.I. Ridley (Eds.), *Applications of Microanalytical Techniques to Understanding Mineralizing Processes: Reviews in Economic Geology*, v. 7, p. 1-35.

Woodhead, J. and Hergt, J., 2007, A Preliminary Appraisal of Seven Natural Zircon Reference Materials for In Situ Hf Isotope Determination: *Geostandards and Geoanalytical Research*, v.29, p.183-195.